TUJNAS
ISSN-Print: 2073-0764
ISSN-Online: 2959-4340

Thamar University Journal of
Natural & Applied Sciences
(TUJNAS)

Journal website:
www.tu.edu.ye/journals/index.php/TUJNAS/index

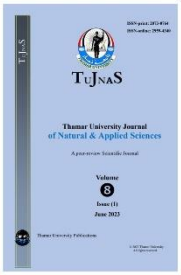

ORIGINAL ARTICLE

Photo-Electrical Tandem of Modulated Polyvinyl Alcohol Based Plasticized Solid Polymer Electrolyte Nanocomposite Films: Effect of Propylene Carbonate Contents

Murad Q. A. Al-Gunaid[1]*, Waled Abdo Ahmed[1], Mohammed. A. dhif-Allah[2], Fares H. Al-Ostoot[3]

Affliations:
[1]Department of Chemistry, Faculty of Education, Thamar University, Dhamar 87246, Yemen

[2]Department of Agriculture, Faculty of Agriculture, Thamar University, Dhamar 87246, Yemen

[3]Department of Biochemistry, Faculty of Education and Science, Al-Baydha University, Al-Baydha, Yemen.

Corresponding Author:
Murad Q. A. Al-Gunaid, emails: morad.jounid11@gmail.com, or MuradAl-Gunaid11@tu.edu.ye

Received: Mar 21, 2023,

Revised Date: Apr 20, 2023,

Accepted Date: May 8, 2023,

Online Date: Jun 12, 2023

Published: Jun 13, 2023

DOI:
https://doi.org/10.59167/tujnas.v8i1.1490

Abstract

Plasticized solid polymeric electrolyte nanocomposites based on polyvinyl alcohol (PVA) incorporating Cs_2CuO_2 nanoparticles (NPs), electrolyte salt ($LiClO_4$) and plasticizer (PC) were prepared via solution casting technique. The dynamic light-scattering histogram revealed that the prepared Cs_2CuO_2 NPs have a size in the range of 80-120 nm. The interaction between different components in PVA/Cs_2CuO_2/$LiClO_4$-PC films (plasticized PVA-SPEs) were probed by FTIR, while the surface and structure were evaluated by SEM and XRD, which indicate to amorphous nature of plasticized PVA-SPEs. The thermal behavior of films was measured via TGA, where a partial decrease in the thermal stability of films was noticed with an increase of PC content in the PVA-SPEs. The highest conductivity achieved is $9.56X10^{-5}$ S/cm for PVA-SPEs containing 8wt% PC at 298K. The plasticized PVA-SPEs exhibited higher specific capacitance by two folds and photovoltaic efficiency by three folds compared to pure PVA matrix.

Keywords

PC; PVA-SPEs; Ac-conductivity; Specific capacitance; Photovoltaic efficiency

1. Introduction

Polymer electrolytes are widely used by researchers in various electrochemical devices as they are flexible and versatile in shape. The advantages of using polymeric electrolytes are concentrated on their desirable characteristics: good compatibility with lithium metal; no leakage; low self-discharge in batteries; relaxing elastically under stress and easy processing with continuous production. However, the low ionic conductivity at ambient temperature is one of the major drawbacks of polymer-based solid polymer electrolytes (SPEs) that limit their practical applications [1, 2]. To overcome these problems, solid polymer electrolyte (SPEs) are incorporated with nanocrystals and plasticizers which meets these criteria. Polymer nanocomposite electrolyte was prepared by dispersing the nanoparticles (NPs) such as CuO, ZnO, TiO_2, Al_2O_3, etc., into a complex matrix of polymers and salts [3-6]. The dispersion of NPs and electrolyte salt in the polymeric matrix is an attractive approach due to assist in modifying (i) the local structure/morphology of the matrix (ii) the crystallinity degree (iii) the glass transition temperature (iv) the flexibility of the polymeric segment (v) the chemical properties of the filler particles and (vi) the interaction between heterogeneous systems of nanocrystals/salt and polymers [7]. Besides, one of the useful methods to improve ionic conductivity is the addition of plasticizers as plasticized polymer electrolytes in the solid form [8-12]. The most used plasticizers are low molecular weight organic solvents such as ethylene carbonate (EC), propylene carbonate (PC), dimethyl carbonate (DMC), diethyl carbonate (DEC) and so on [13, 14]. The addition of plasticizer into SPEs leads to enhance the ionic conductivity of 1-2 orders magnitude by increasing flexibility as well as the amorphous content of polymer electrolytes, dissociating salt into free ions, a significant change in morphological structure and lowering the glass transition temperature, Tg [7, 15].

In the current new field, there is always demand for light, safe, and economical devices, so researchers are focusing on the production of such devices whose storage, production and distribution are preferentially at low cost. In this regard, hydrophilic polyvinyl alcohol (PVA) is a potential host polymer having high dielectric strength, good charge storage capacity, high suitable film forming and good mechanical properties [16, 17]. Thus; it has been investigated as they are abundantly available, economical and biodegradable. PVA shows high transparency, compatibility and adhesiveness to the electrode so can be used in electrochemical devices such as cells, sensors, optical devices, etc.

The fine structure of $LiClO_4$ enhances its solubility in the polymer matrix and, eventually, speeds up the salt dissociation process. $LiClO_4$ is used due to its abundant availability, water-soluble and also eco-friendly. Propylene carbonates (PC) have a high

dielectric property and it is a good solvent for electrolyte salt. The plasticizer has an important role towards enhances the segmental motion of PVA chains associated with an increase in the ionic charge carries by increasing the dissociation of electrolyte salt. It restricts the dissociated ions from the salt reforming process and reduces the agglomeration of particles inside the matrix which assist in the performance homogeneity dispersion of components in composite films. Subsequently, the polarization particles inside the composite will increase, reflex in an improve the electrical permittivity and capacity of the stored energy of composite films by reducing the potential barrier in front of the mobility of Li^+ among polymer chains, hence the ionic conductivity will increase. Therefore, the target of the current work is an attempt is made to investigate with enhance the electrical, electrochemical, and optical efficiency of flexible PVA-SPE films and explore the effect of propylene carbonate contents on the features of such films.

2. Experimental Details

2.1 Materials

PVA (average molecular weight 125,000 Aldrich), lithium perchlorate tri hydrate ($LiClO_4.3H_2O$), propylene carbonate as a plasticizer, (PC) ($C_4H_6O_3$) (AR grade, SD. Fine chem.,). Both cesium nitrate ($CsNO_3$), copper (II) nitrate trihydrate [$Cu(NO_3)_2.3H_2O$] (as oxidants) and glycine ($C_2H_5NO_2$) (as fuel) and were purchased from (SD fine-chem, Mumbai, India). Double distilled water was used as a solvent in this study.

2.2 Synthesis Cs_2CuO_2 NPs

In this study, cesium copper oxide Cs_2CuO_2 NPs was synthesized with the sol-gel auto combustion method [18, 19]. AR-grade $Cu(NO_3)_2.3H_2O$, $CsNO_3$, and glycine ($C_2H_5NO_2$; fuel) were weighed in stoichiometric proportions and dissolved in double-distilled water. The molar ratio of the fuel to the oxidant nitrates was 2:1. The individual solutions were then mixed together, and the pH value was adjusted to 8.5 by the addition of NaOH solution. Then, the solution was stirred continuously at 90°C for 2hrs to obtain the gel. The gel was heated until the combustion process occurred, and a loose powder was formed. Finally, the dark grayish brown powder was calcinated at 650-800°C for 2hrs.

2.3 Casting of plasticized PVA-SPEs

PVA of 21g obtained in the powder form was dissolved in 300 ml of doubly distilled water at 80°C for about 2hrs. The 10wt% of $LiClO_4$ was added separately four times into four beakers containing 50 ml of PVA solutions to form polymer electrolyte solutions and then stirred for 1 hr by using a magnetic stirrer at room temperature. Calculated amount viz., 2, 4, 6 and 8wt% of PC and added to the previous solutions separately with continuous stirring for1hr,

then 2wt% of Cs_2CuO_2 NPs added to each of the above-plasticized polymer electrolyte solutions with stirred for 30 min and sonicated for 30min. The plasticized PVA-SPEs were cast in a four petri-dish and the solvent evaporated at room temperature. For complete removal of solvent, the samples were vacuum dried in a hot air oven at 60 ˚C for 4-6 hrs. The thickness of obtained films varied from 0.20 to 0.23 mm. The chemical structure of the pure PVA matrix and the schematic of the composite were depicted in Figure 1.

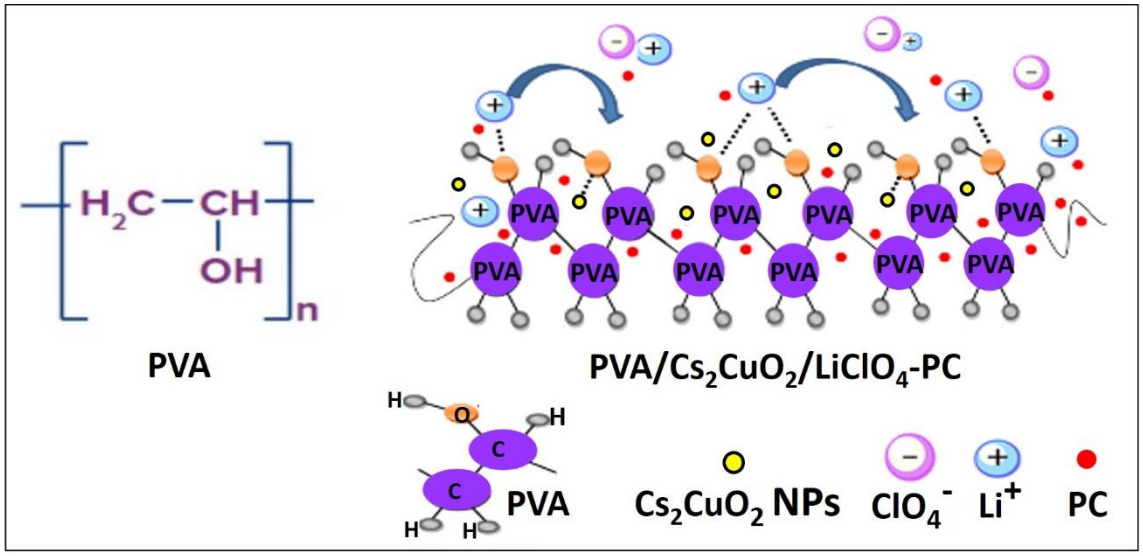

Figure 1. Chemical structure of pure PVA and schematic representation of PVA/Cs_2CuO_2/$LiClO_4$- PC film.

2.4 Techniques

The size of Cs_2CuO_2 NPs was measured by dynamic light scattering (Zetasizer Nano ZS, Malvern Instruments, United Kingdom). The morphological behaviors of plasticized PVA-SPEs were recorded with a Zeiss-108A scanning electron microscope (SEM), in Germany. The structure of pristine Cs_2CuO_2 NPs and plasticized PVA-SPE films were obtained at room temperature by X-ray diffraction (XRD) on a D8 Advance-Bruckers AXS diffractometer with Cu-Kα radiation source (λ = 1.54 ˚A), operated at 40 kV and 40 mA in the 2θ range 10-80˚ at the scan speed of 0.05˚ per second. The physical interaction between components was studied by Fourier transform infrared (FTIR) spectroscopy, JASCO 4100 spectrometer, Japan. All samples scanned over the wave number range 4000-500 cm^{-1}.

The ac-electrical and current-voltage (I-V) features of films were measured by LCR-meter, Wayane Kerr-6430, UK at room temperature. The ac-electrical studies have been carried out in the frequency range 50 Hz-5MHz at 1V. The surface of the films was coated with silver paste and sandwiched between two stainless steel electrodes which had an area of 0.5 cm^2.

Electrochemical cyclic voltammetry (CV) was performed using CH Instrument, model 600D series, with potassium hydroxide (2M) as the background electrolyte at a potential scan rate of 0.1 $V.s^{-1}$, using Ag/AgCl reference and platinum wire as counter electrodes. The photovoltaic (PV) solar-based test system was estimated by Keithley, 2400 digital source meters, Japan with 450 W xenon light source under sun-powered light illumination intensity (60 $mWcm^{-2}$). For the preparation of the photoanode cell, TiO_2 glue was spread over the conducting surface of FTO (1 X 1 cm^2) to make a substrate film of ~ 10 mm thickness.

The dried slide was drenched in a natural pomegranate dye and dried for 2 hrs with a compressed air gun. Another bit of FTO-covered with carbon black. The plasticized PVA-SPE films were immersed in the electrolyte solution (KI/I_2 in ethylene glycol) for 10 min followed by being sandwiched between the two FTO glasses. The sandwiched plasticized PVA-SPEs with two FTO glasses were immersed in electrolyte for a few minutes and then utilized for DSSC studies. The thermal stability of the plasticized SPEs has been studied using thermogravimetric analysis (TGA), TA Instrument Q600, USA, in the temperature range of 30 – 800 ˚C with the heating rate of 15 ˚C/min, in nitrogen gas flow rate of 50 cm^3/min.

3 Results and discussion

3.1 Structural& morphological studies

Figure 2 (a-f) displays the X-ray diffraction (XRD) patterns of pristine Cs_2CuO_2 NPs, pure PVA and different plasticized SPE films. Addition of plasticizer, PC to $PVA/Cs_2CuO_2/LiClO_4$ has been observed to result in an increase in the amorphous nature.

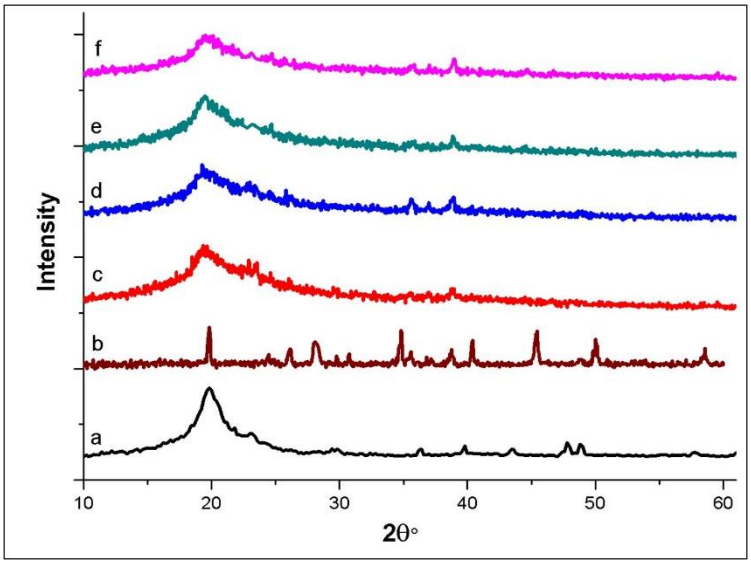

Figure 2. XRD patterns of; a) PVA, b) Cs_2CuO_2 NPs, $PVA/Cs_2CuO_2/LiClO_4$ with c) 2, d) 4, e) 6 and f) 8wt% PC.

As presented in Figure 2(a), PVA has a characteristic peak at 2θ = 19.8° referred to the semi-crystalline nature of PVA [20]. Whereas the pristine Cs_2CuO_2 NPs exhibit multi-sharp crystalline peaks at 2θ of 19.7, 26.1, 28.1, 34.7, 46.2, and 50.18° (Figure 2 (b)). The peaks corresponding to PVA and Cs_2CuO_2 NPs significantly reduced with the addition of PC and $LiClO_4$ in SPEs (Figure 2(c-f)). The addition of PC caused to increase in the dissociation of Li salt, which in turn increases in the interaction between components in SPE films [21]. Therefore, the intensity of the peak at 2θ = 19.8°was decreased and becomes wider in the plasticized PVA-SPE films. Such a decrease in the crystallinity of plasticized PVA-SPE films is in accord with the ionic conductivity results.

Figure 3(a) displays the dynamic light-scattering histogram for the Cs_2CuO_2 NPs, and it reveals that the prepared NPs size was in the range of 80-120nm. The surface morphology and distribution of Cs_2CuO_2 NPs, Li salt and PC in the PVA matrix were characterized using SEM as presented in Figure 3(b-f).

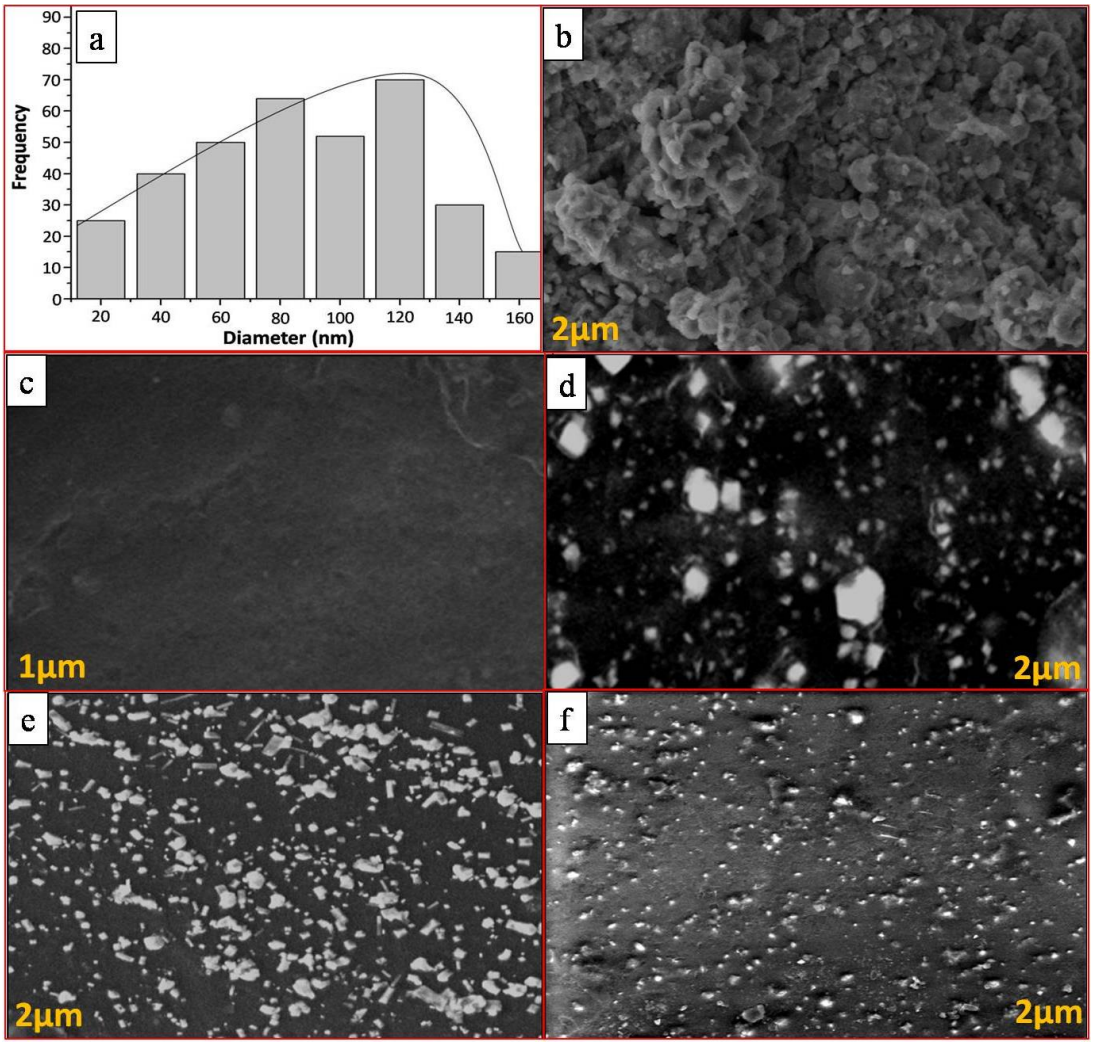

Figure 3. a) Dynamic light-scattering of Cs_2CuO_2 NPs, SEM photomicrographs of; b) pristine Cs_2CuO_2, c) pure PVA, PVA/Cs_2CuO_2/ $LiClO_4$ with d) 2, e) 4 and f) 8wt% PC.

SEM image of the Cs_2CuO_2 NPs shows a porous, agglomerated, and spherical-like structure which was reported else in previous literature [22]. From Figure 3 (c), the SEM image of pure PVA shows a soft surface without any cracks. Besides, the presence of almost spherical NPs and Li salt in the PVA matrix has a uniform distribution with increasing the different amounts of PC in SPEs (Figure 3 (d-f)). These results indicate that the Li salt becomes more dissociation and the NPs have less agglomerated with increasing the PC contents. The addition of PC which has high dielectric constant acts as a solvent for Li salt and prevents NPs from agglomerating in PVA-SPEs. That leads to finer dispersion of fillers in the PVA matrix and the surface of plasticized PVA-SPE films becomes less rough as shown in the films containing 8wt%PC (Figure 3 (e)).

3.2 FTIR analysis

The FTIR analysis provides a powerful means to characterize the complex formation in plasticized PVA-SPE films. Figure 4 displays FTIR spectra for pure PVA and its NCs with 2, 4, 6 and 8 % of PC.

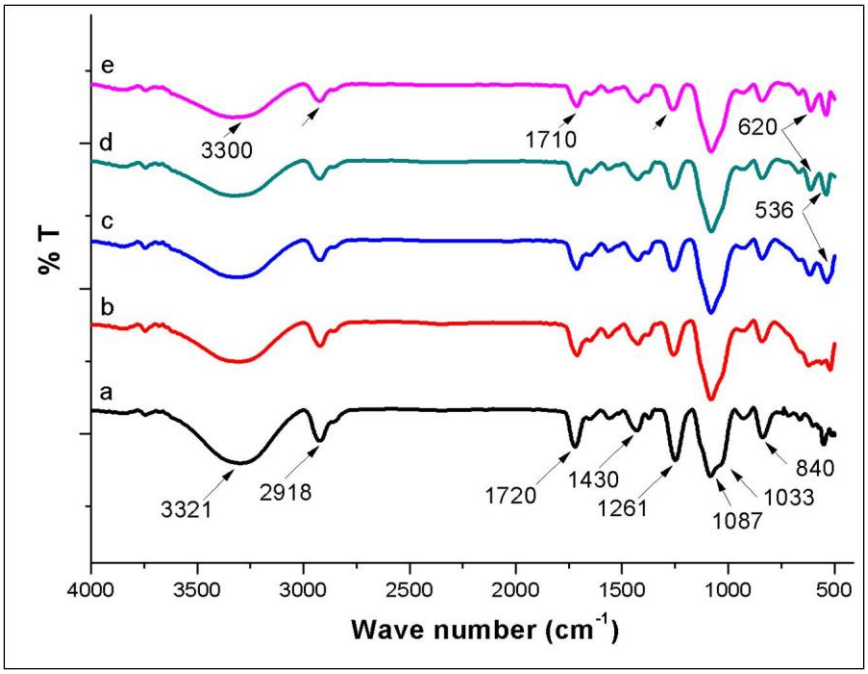

Figure 4. FTIR spectra for a) pure PVA, PVA/Cs_2CuO_2/$LiClO_4$ SPEs with b) 2, c) 4, d) 6 and d) 8wt % of PC.

The reduction in the peak's intensity at 3321, 2918, 1720, 1430, 1260 and 1033 cm^{-1} are assigned to the effect of fillers NPs, Li salt and different amounts of PC [23, 24]. The broad peaks at 3320 and 1087-1033 cm^{-1} referred to the stretching of hydroxyl groups and the single

bond C-O, respectively of the PVA matrix. These peaks exhibited partially changed in plasticized PVA-SPEs. The reducing intensity of both –OH and C-O peaks with the absence of a small shoulder at 1033 cm^{-1} after added PC content confirms the interaction between the fillers and oxygen atoms in the PVA structure.

Further, the intensity of the stretching vibration peak of -CH_2- in PVA-SPEs at 2918 cm^{-1} is decreased because of the existence of Li salt, NPs and PC contents. The reduced intensity of the vibrational peak corresponds to 1720 cm^{-1} with increasing PC content was noticed, which refers to the physical interaction between the carbonyl group of residual acetate groups in the PVA structure with Li^+ of the dissociation salt. A slight decrease of bending vibration in-plane at 1430 cm^{-1} and out-of-plane at 840cm^{-1} of -CH_2 in PVA was observed [25]. There are two peaks were noticed at 620 and 536cm^{-1}, which may be attributed to the effect of inorganic metal oxide NPs [26]. The above observations of reduction in intensity, broadening and shifting of the vibrational peaks confirm the complex formation between Li salt, Cs_2CuO_2 NPs and PVA with increasing the PC contents in SPE films.

3.3 Thermal studies

Figure 5 illustrates the typical thermograms for the decomposition process of PVA and its plasticized PVA-SPE films. The thermal stability revealed through TGA thermograms for plasticized PVA-SPE films is generally significantly lower than that of pure PVA entity. The PVA matrix has adequate stability in the temperature range of 30-330 $^{\circ}$C, then the main decomposition process occurs in the temperature range of 330-500°C, with a weight loss of around 88wt%. From Figure 5, it can be observed that the change in baseline on TGA curves for all PVA-SPE films in the temperature range of 50-200 $^{\circ}$C. It may have referred to the evaporation of adsorbing bulk water and low boiling point components with 6.7wt % loss of pure PVA and 15.6 wt% for 8wt% PC-loaded SPE. As expected, the increasing PC content in the PVA-SPEs causes a reduction in the thermal stability of films accompanied by weight loss from composites at different temperature ranges. Such behavior indicates the incorporated PC into PVA-SPE films leads to a partially reduced thermal stability and the films become flexible and more amorphous. Similar behavior of the effect of plasticizer on the thermal stability of SPE films was published else in the literature [27, 28].

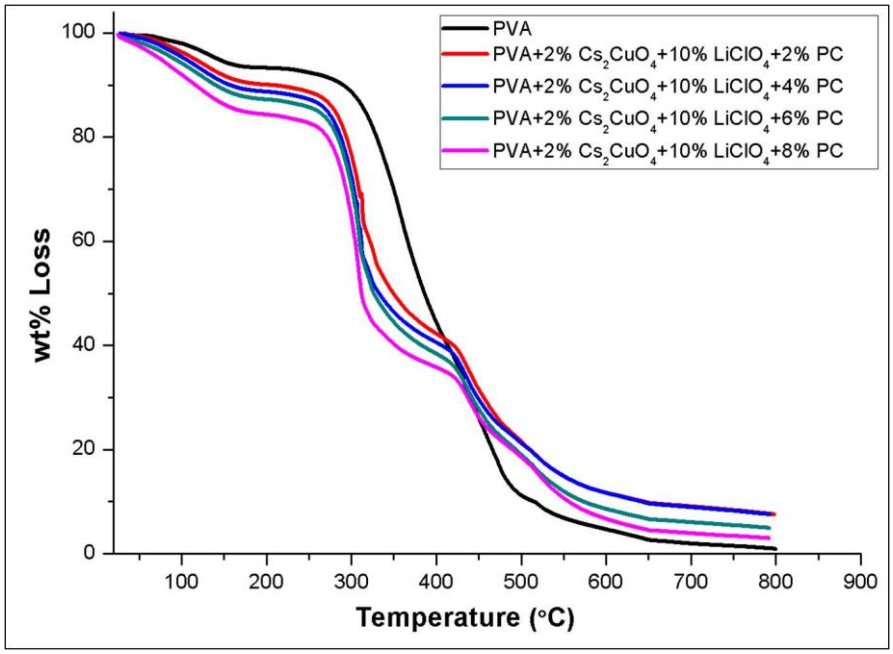

Figure 5. TGA Thermograms of PVA/Cs_2CuO_2/$LiClO_4$-PC versus temperature.

3.4 Electrical and electrochemical behaviors

The ac-conductivity, σ_{ac} versus PC contents in PVA-SPEs at different frequencies and the room temperature were displayed in Figure 6 (a). At lower frequency and less PC content, the σ_{ac} was low. The space charge polarization or impedance of the electrolyte at the electrode/electrolyte interface describes the lower-frequency region of conductivity [29, 30]. In lower frequency regions, the charge carriers are accumulating and stay relatively for a long time at the electrode/electrolyte interface because of the polarization of the electrode. Therefore, the mobility of ions is hindered by these accumulated charges due to columbic repulsion, consequently less ionic conductivity. At higher frequencies, the charge carriers (Li^+ ions) gain more energy and that leads to increasing their mobility through the PVA matrix which becomes more flexible with increasing PC content [31]. As PC content increases, the dissociation of lithium salt will increase means more Li^+ ions will exist, while the viscosity and crystallinity of the PVA matrix will be reduced. Therefore, the segmental motion and flexibility of polymeric chains assist in the transportation of Li^+ ions through the PVA matrix, hence σ_{ac} increase [32]. The maximum σ_{ac} value at higher frequency was found as $9.56X10^{-5}$ S/cm for PVA-SPE doped with 8wt% of PC, however; it is around 0.017, 1.39, 2.21 and 4.95 $X10^{-5}$ S/cm for pure PVA, PVA-SPE doped with 2, 4 and 6wt% of PC, respectively.

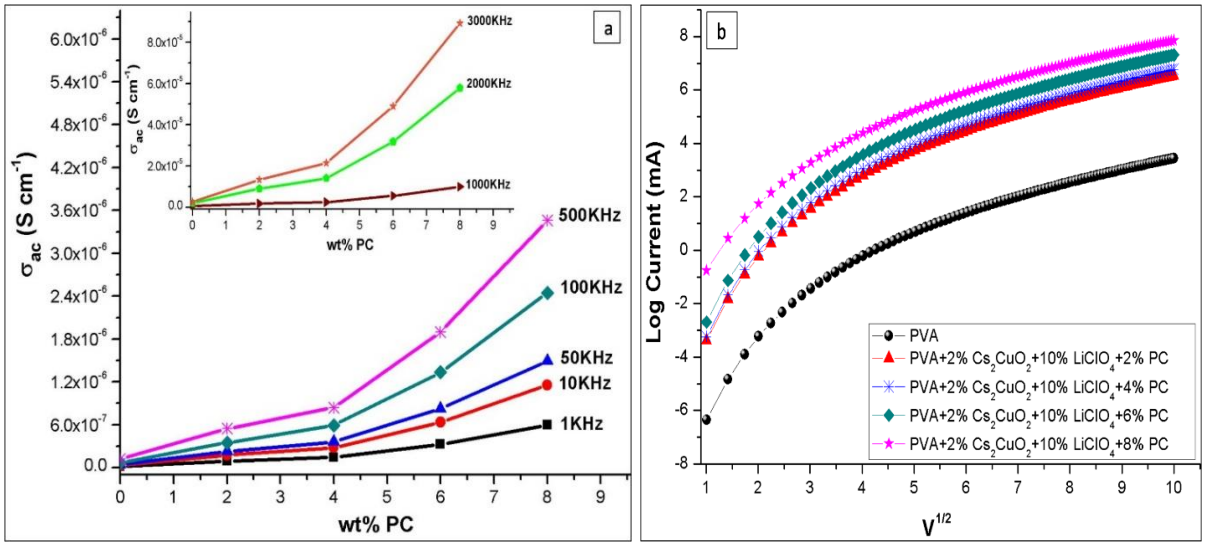

Figure 6. Plots of; a) Ac-conductivity versus PC content at different frequencies and b) Log I versus $V^{1/2}$ of PVA-SPEs.

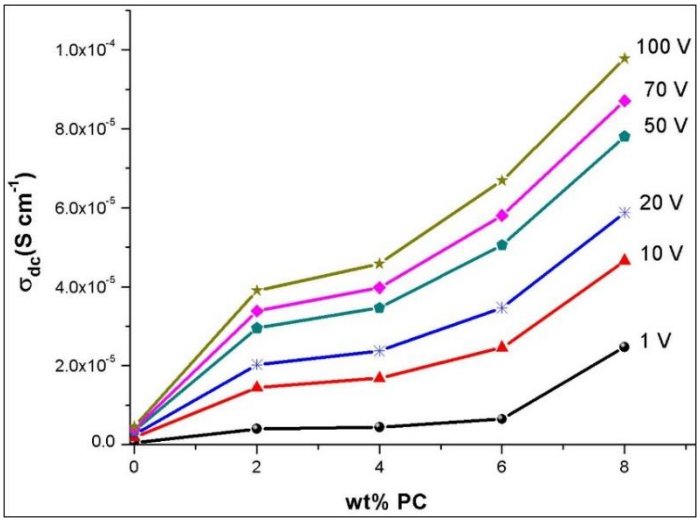

Figure 7. Dc-conductivity versus PC content of PVA-SPEs at different voltages.

Furthermore, in order to determine the exact charge transport mechanism of dc-conductivity in plasticized PVA-SPEs, the plots of log (I) versus ($V^{1/2}$) were plotted as shown in Figure 6 (b). For the Schottky mechanism, the plots of log (I) versus ($V^{1/2}$) should have fit linear plots without deviation [33]. In the current case, the deviation in linearity is observed at below < 4V, therefore the Schottky mechanism was ruled out. Such nonlinear characteristics can arise from transport processes of the number of non-ohmic charge carriers. The deviation of plots may indicate the Poole-Frenkel mechanism, where the transport of charge carriers arises from the electrons of NPs accompanied by the hopping of Li^+ ions through the PVA chains.

Figure 7 showed the dc-conductivity, σ_{dc} dependence on the PC content, which is embedded in PVA-SPE films at room temperature. The increase in σ_{dc} with increasing PC loadings was noticed at different voltages and sharply increases at higher voltages. The increase in PC contents means the small molecules will penetrate into PVA chains and separates them from each other; as a result, the free volume becomes more. That enhances the flexibility and the segmental motion of PVA chains. Besides that, the degree of dissociation of Li salt increases with an increase in the dosage of PC, which leads to enhancement in the σ_{dc}.

Cyclic voltammetry (CV) has been carried out between sweep potential and charge to evaluate the electrochemical stability of the plasticized PVA-SPE films. Figure 8 displayed CV curves of plasticized PVA-SPE films, which have a semi-rectangular shape with a higher current density as compared with pure PVA. The semi-rectangular shape indicates electrochemical stability without decomposition of the films under applied potential voltages.

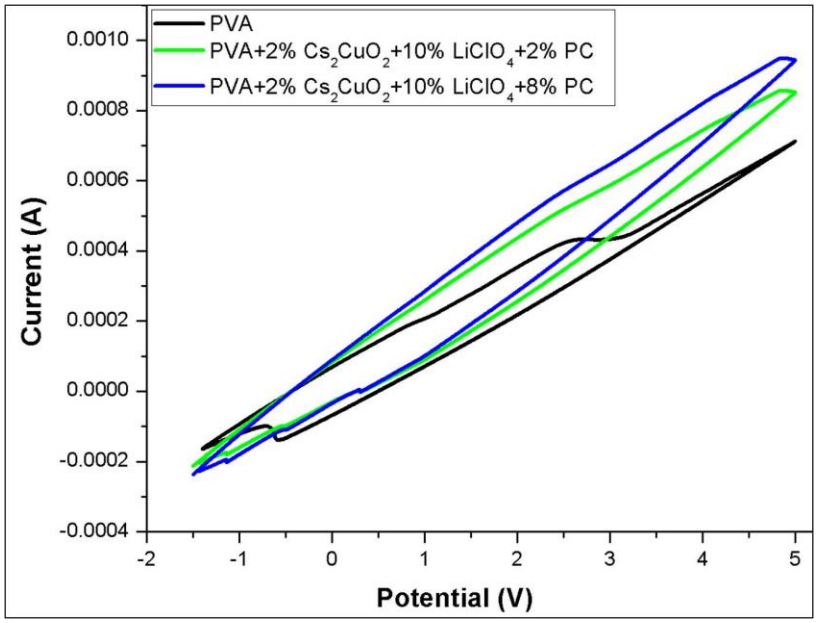

Figure 8. Cyclic voltammetric profiles for PVA and PVA/Cs_2CuO_2/$LiClO_4$-PC SPEs at scan rate of 0.1 $V.s^{-1}$.

The introducing of PC into PVA/Cs_2CuO_2/$LiClO_4$ SPEs leads to producing a flexible film due to the plasticizing effect of PC which also enhances the dissociation of Li salt and the degree of dispersion of fillers. Hence, the interfacial contact is improved leading to an increase in the energy storage of doped films. The improvement of interfacial contact could then induce higher capacitive performance of plasticized SPE films. Furthermore, the ionic conductivity is enhanced upon the addition of a PC which helps in improving the charge storage capacitive behavior. The calculated specific capacitance, C_{spec} of plasticized PVA-SPE films doping with

2 and 8wt% of PC are 3.73 and 4.17 F/g, respectively which is higher than that of pure PVA (2.11F/g). That indicates the addition of PC to PVA-SPE films enhances its capacitance values. The obtained data of the C_{spec} of plasticized PVA-SPE films is higher by two folds compared with the C_{spec} of other PVA nanocomposites reported else [34, 35].

3.5 Photovoltaic activity

Figure 9 shows the photocurrent density-voltage curves for the dye-sensitized solar cells (DSSCs) created for pure PVA and PVA-SPEs containing 2,4 and 8wt% of PC.

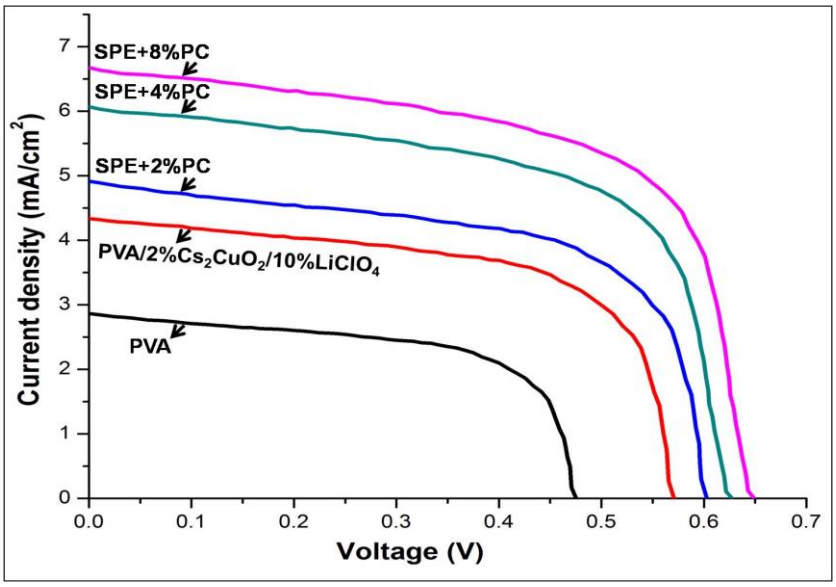

Figure 9. Current density-voltage of pure PVA and PVA/Cs_2CuO_2/$LiClO_4$-PC SPEs in KI/I_2 electrolyte based DSSC under illumination intensity of 60 mW/cm^2.

The Photovoltaic parameters based on DSSCs as the fill factor (*FF*) and the power conversion efficiency (η) for PVA-SPEs were obtained from Eq.1 as follows.

$$FF = \frac{I_{mp} \times V_{mp}}{I_{SC} \times V_{OC}} \quad , \quad \eta(\%) = \frac{FF \times I_{SC} \times V_{OC}}{P_{in}} \times 100\% \qquad (1)$$

Where V_{oc} is the open circuit voltage (V), I_{sc} is the short circuit current density (mA/cm^2), P_{in} is the incident light power, I_{mp} (mA/cm^2) and V_{mp} (V) are the current density and voltage at the maximum point of power output (P_{max}), respectively. The calculated photovoltaic parameters for PVA and PVA-SPE films were listed in Table 1.

Table 1: Photovoltaic parameters of PVA and PVA/Cs2CuO2/LiClO4-PC SPEs based DSSC.

Composition	I_{sc} (mA)	V_{oc} (V)	P_{max}		FF	% FF	% η*
			I_{mp}	V_{mp}			
PVA	2.881	0.471	1.813	0.421	0.562	56.2	1.27
PVA/2%Cs_2CuO_2/10%$LiClO_4$	4.359	0.567	3.316	0.461	0.618	61.8	2.54
PVA/2%Cs_2CuO_2/10%$LiClO_4$+2%PC	4.934	0.601	3.725	0.494	0.621	62.1	3.06
PVA/2%Cs_2CuO_2/10%$LiClO_4$+4%PC	6.106	0.623	4.497	0.538	0.636	63.6	4.03
PVA/2%Cs_2CuO_2/10%$LiClO_4$+8%PC	6.701	0.630	4.791	0.566	0.642	64.2	4.51

*% η is calculated at P_{in} = 60 mW/cm^2.

The results reveal drastic increases in the *FF* and *η* values for the PVA-SPE containing different dosages of PC contents compared to the pure PVA matrix. The increases of *FF* and *η* denote the increase of I_{sc} values through the cell as can be seen in Table 1. The incorporation of 2wt% of Cs_2CuO_2 NPs and10%wt of $LiClO_4$ into the PVA matrix will improve its response towards the absorption of the light and will build a network or conduction path through PVA which facilitates the transportation of charge carriers through it. These movements of charge carriers will aid to separate the opposite charges through the cell. It is clearly noticed that increasing the PC contents in PVA-SPEs leads to an increase in the dissociation of Li salt and will prevent them from reforming salt again as well as restraining the agglomerate of Cs_2CuO_2 NPs in the matrix. The flexibility of PVA-SPEs also will be enhanced after the addition of PC caused to assist the transportation of charge carriers. Besides, the plasticized PVA-SPEs have higher conductivity compared to the insulating pure PVA. Therefore, the plasticized PVA-SPEs have higher *FF* and *η* values than other formulations. Additionally, the higher ionic mobility of iodide ions of electrolyte and the faster re-excited of the electrons from HUMO to LUMO from the dye orbital leads to improvement in the efficiency of the cell. The *η* value of pure PVA (1.27 %) in iodide electrolyte in this study is very close to that for pure PVA/KI/I_2 (1.97 %) reported in the literature [36, 37]. While the *η* value of PVA-SPE containing 8wt% of PC (4.51 %) is higher by one-fold than that of PVA/4 wt% α-Fe_2O_3 (3.62 %) NC in the KI/I_2, published elsewhere [38, 39]. Such outcomes demonstrate that the plasticized PVA-SPEs can be improved to widen their potential application as a promising flexible material for DSSCs.

4 Conclusions

The plasticized PVA-SPEs containing different dosages viz., 2, 4, 6 and 8 wt% of PC as a plasticizer have been fabricated by the solution-casting method. The XRD and SEM analysis confirmed a significant microstructural variation and uniform dispersion of fillers in SPEs respectively, whereas the dispersion becomes more ideal with increasing PC content in SPE films. FTIR spectroscopy further established that the incorporation of varying amounts of PC in SPEs changes the vibration stretching peaks of main groups in the PVA matrix as a result of increasing the ion-dipole interactions. The ac and dc conductivity increases with increasing the frequency and PC contents in PVA-SPEs. The Pool-Frenkel mechanism associated with the ions hopping is found to be the dominant conduction mechanism responsible for charge transport. In plasticized PVA-SPE films, the interfacial contact between electrode-electrolyte and mobility of ions leads to enhance their specific capacitance. TGA studies revealed that the addition of 8 wt% PC in the NC films shifts the thermal decomposition temperature to a lower value. The photovoltaic efficiency of plasticized PVA-SPEs increases by two folds compared with pure PVA and that may be adjustable to widen their potential application in DSSCs.

References

[1] Cha E. H., Macfarlane D. R., Forsyth M. and Lee C. W., (2004) Ionic Conductivity Studies of Polymeric Electrolytes Containing Lithium Salt with Plasticizer, *Electrochimica Acta* **50:** 335-338.

[2] Jinisha B., Anilkumar K. M., Manoj M., Pradeep V. S. and Jayalekshmi S., (2017) Development of A Novel Type of Solid Polymer Electrolyte for Solid State Lithium Battery Applications Based On Lithium Enriched Poly (Ethylene Oxide) (PEO)/Poly (Vinyl Pyrrolidone) (PVP) Blend Polymer, *Electrochimica Acta* **235:** 210-222.

[3] Arup D., Kajari D. S., Karan S. and De K. (2011) Vibrational Spectroscopy And Ionic Conductivity of Polyethylene Oxide–$NaClO_4$–CuO Nanocomposite, *Spectrochimica Acta Part A: Molecular and Biomolecular Spectroscopy* **83:** 384-391.

[4] Patil S. U., Yawale S. S. and Yawale S. P. (2014) Conductivity Study of PEO–$LiClO_4$ Polymer Electrolyte Doped with ZnO Nanocomposite Ceramic *Filler*, *Bulletin of Materials Science* **37:** 1403-1409.

[5] Vignarooban K., Dissanayake M.A.K.L., Albinsson I. and Mellander B. E. (2014) Effect of TiO_2 Nano-Filler And EC Plasticizer on Electrical And Thermal Properties of Poly(Ethylene Oxide) (PEO) Based Solid Polymer Electrolytes, *Solid State Ionics* **266:** 25-28.

[6] Das S. and Ghosh A. (2015) Ion Conduction and Relaxation in PEO-LiTFSI-Al_2O_3 Polymer Nanocomposite Electrolytes, *Journal of Applied Physics* **117:** 174103 (1-7).

[7] Pradan D.K., Samantaray B.K., Choudary R. N. P. and Thakur A.K. (2005) Effect of Plasticizer on Structure-Property Relationship in Composite Polymer Electrolytes, *Journal of Power Sources* **139**: 384-393.

[8] Xiaofei M., Jiugao Y., and Wang N. (2007) The Effects of Different Plasticizers on the Properties of Thermoplastic Starch as Solid Polymer Electrolytes, Macromolecular *Materials and Engineering* **292:** 503-510.

[9] Pradhan D. K., Choudhary R. N. P., K.Samantaray B., Karan N. K. and Katiyar R. S. (2007) Effect of Plasticizer on Structural and Electrical Properties of Polymer Nanocompsoite Electrolytes, *International Journal of Electrochemical Science* **2:** 861-871.

[10] Pitawala H. M. C., Dissanayake M. A. L., Seneviratne V. A., Mellander B. E. and Albinson I. (2008) Effect of Plasticizers (EC or PC) on The Ionic Conductivity and Thermal Properties of the $(PEO)_9LiTf:Al_2O_3$ Nanocomposite Polymer Electrolyte System, J. Solid State Electrochemistry **12:** 783-789.

[11] Pawlicka A., Danczuk M., Wieczorek W. and Monikowska E.Z. (2008) Influence of Plasticizer Type on The Properties of Polymer Electrolytes Based on Chitosan. *The Journal of Physical Chemistry A* **112**: 8888-8895.

[12] Sasithorn K. and Jantrawan P. (2015) Effects of Nano Alumina and Plasticizers on Morphology, Ionic Conductivity, Thermal and Mechanical Properties of PEO-$LiCF_3SO_3$ Solid Polymer Electrolyte, *Electrochimica Acta* **161**:171-176.

[13] Zhao H., Park S. J., Feifei S., Yanbo F., Battaglia V., Philip N. R. J. and Liu G. (2014) Propylene Carbonate (PC)-Based Electrolytes with High Coulombic Efficiency For Lithium-Ion Batteries, *Journal of the Electrochemical Society* **161**: 194-200.

[14] Shukur M. F., Majid N. A., Ithnin R. and Kadir M. F. Z. (2013) Effect of Plasticization on the Conductivity and Dielectric Properties of Starch–Chitosan Blend Biopolymer Electrolytes Infused with NH_4Br, *Physica Scripta* **157**: 014051(1-6).

[15] Anupama B.H., Murad Q. A. A, Shashikala B.S., Somesh T.E., Kavya R., Siddaramaiah and Madhukar B.S. (2023) Poly (O-Anicidine) Encapsulated K_2ZrO_3 Nano-Core Based Gelatin Nanocomposites: Investigation of Optical, Thermal, Microcrystalline and Morphological Characteristics, *Chemistry Select* **7**: 1-12.

[16] Rajeswari N., Selvasekarapandian S., Karthikeyan S., Sanjeeviraja C., Iwai Y. and Kawamura J. (2013) Structural, Vibrational, Thermal, and Electrical Properties of PVA/PVP Biodegradable Polymer Blend Electrolyte with CH_3COONH_4, *Ionics* **19**: 1105-1113.

[17] Radha K., Selvasekarapandian S., Karthikeyan S., Hema M. and Sanjeeviraja C. (2013) Synthesis and Impedance Analysis of Proton-Conducting Polymer Electrolyte PVA:NH_4F, *Ionics* **19**: 1437-1447.

[18] Murad Q.A.A., Adel M.N.S., Subramani N.K., Madhukar B. S. and Siddaramaiah (2017) Optical Parameters, Electrical Permittivity and I-V Characteristics of PVA/Cs_2CuO_2 Nanocomposite Films for Opto-Electronic Applications, *Journal of Materials Science: Materials in Electronics* **28**: 8074-8086.

[19] Anupama B.H., Murad Q.A. A. and Siddaramaiah (2021) Performance of Nano-K-doped Zirconate On Modified Opto-Electrical and Electrochemical Properties of Gelatin Biopolymer Nanocomposites, *Polymer Bulletin* **78**: 3023-3041.

[20] Somesh T. E, Murad Q.A. A., Madhukar B.S. and Siddaramaiah (2018) Photosensitization of Optical Band Gap Modified PVA Films with Hybrid $AgAlO_2$ Nanoparticles, *Journal of Materials Science: Materials in Electronics* **30**: 37-49.

[21] Sharma J. P. and Sekhon S. S. (2013) Effect of Plasticizer and Fumed Silica on Ionic Conductivity Behavior of Proton Conducting Polymer Electrolytes Containing HPF_6, *Bulletin of Materials Science* **36:** 629-634.

[22] Murad Q.A. A., Adel M. N. S. and Siddaramaiah (2018) Effects of the Electrolyte Content on The Electrical Permittivity, Thermal Stability, and Optical Dispersion of Poly (Vinyl Alcohol)–Cesium Copper Oxide–

Lithium Perchlorate Nanocomposite Solid-Polymer Electrolytes, *Journal of Applied Polymer Science* **135**: 45852(1-14).

[23] Osman Z., Ansor N. M., Chew K.W. and Kamarulzaman N. (2005) Infrared and Conductivity Studies on Blends of PMMA/PEO Based Polymer Electrolytes, *Ionics* **11**: 431-435.

[24] Adel M.N S., Murad Q.A. A. and Siddaramaiah (2018) Effect of Lithium Perchlorate on the Optoelectrical and Thermal Properties of Poly (Vinyl pyrrolidone)/Nano-Cesium Aluminate Solid Polymer Electrolytes, *Polymer Plastics Technology and Engineering* **57**: 1554-1566.

[25] Papke B.L., Ratner M. A. and Shriver D. F. (1981) Vibrational Spectroscopy and Structure of Polymer Electrolytes, Poly (Ethylene Oxide) Complexes of Alkali Metal Salts, *Journal of Physics and Chemistry of Solids* **42**: 493-500.

[26] Karthik K., Victor J., Kanagaraj M. and Arumugam S. (2011) Temperature-Dependent Magnetic Anomalies of CuO Nanoparticles, *Solid State Communications* **151**: 564-568.

[27] Adel M. N. S., Hezam A., Murad Q. A. A., Somesh T.E. and Siddaramaiah (2020) Effect of Ethylene Carbonate on Properties of PVP-$CsAlO_2$-$LiClO_4$ Solid Polymer Electrolytes, *Polymer-Plastics Technology and Materials* **60**: 132-146.

[28] Murad Q. A. A., Shashikala B.S., Gayitri H.M., Khaled A., Nabil A., Ahmed B. and Fares H. A. A. (2022) Characterization of Opto-Electrical, Electrochemical and Mechanical Behaviors of Flexible PVA/(PANI+La_2CuO_4)/$LiClO_4$-PC Polymer Blend Electrolyte Films, *Macromolecular Research* **30**: 1-9.

[29] Ramesh S., Yin T. S. and Liew C-W. (2011) Effect of Dibutyl Phthalate as Plasticizer on High Molecular Weight Poly (Vinyl Chloride) Lithium Tetraborate Based Solid Polymer Electrolytes, *Ionics* **17**: 705-713.

[30] Murad Q.A. A., Adel M.N.S., Gayitri H. M. and Siddaramaiah (2020) Impact of Nano-Perovskite La_2CuO_4 on Dc-Conduction, Opto-Electrical Sensing and Thermal Behavior of PVA Nanocomposite Films, *Polymer-Plastics Technology and Materials* **59**: 469-483.

[31] Elias S. and Mohd A. M. (2006) Effect of Radiation on Conductivity of Solid PVA–KOH–PC Composite Polymer Electrolytes, *Ionics* **12**: 53-56.

[32] Rajendran S., Sivakumar M., Subadevi R. (2004) Investigations on The Effect of Various Plasticizers in PVA-PMMA Solid Polymer Blend Electrolytes, *Materials Letters* **58**: 641-649.

[33] Murad Q.A. A., Somesh T.E, Gayitri H.M, Fares H. Al-Ostoot and Siddaramaiah (2020) Optimized Nano-Perovskite Lanthanum Cuprate Decorated PVA Based Solid Polymer Electrolyte, *Polymer-Plastics Technology and Materials* **59**: 215-229.

[34] Gayitri H. M., Murad Q.A. A., Siddaramaiah, and Gnana P. A. P. (2020) Investigation of Triplex $CaAl_2ZnO_5$, Nanocrystals on Electrical Permittivity, Optical and Structural Characteristics of PVA Nanocomposite Films, *Polymer Bulletin* **77**: 5005-5026.

[35] Gayitri H. M., Murad Q. A. A., Fares H. A., Nabil A., Ahmed B., and Gnanaprakash A.P. (2023) Investigation on Opto-Electrical Structural And Electrochemical Performance of PVA/$ZnBi_2MoO_7$ Hybrid Nanocomposites, *Polymer Bulletin* **80**: 773-790.

[36] Arof A. K., Naeem M., Hameed F., Jayasundara W. J. M., Careem M. A., Teo L. P. and Buraidah M. H. (2014) Quasi Solid State Dye-Sensitized Solar Cells Based On Polyvinyl Alcohol (PVA) Electrolytes Containing I^-/I^{-3} Redox Couple, *Optical and Quantum Electronics* **46**: 143-154.

[37] Shashikala B. S., Murad Q.A. A., Somesh T.E, Siddaramaiah and Anasuya S. J. (2022) Core-Shell Synergistic Effect of (PANI-$NaBiO_2$) Incorporation Polycarbonate Films to Photodegradation of MG Dye and Photovoltaic Activity, *Polymer Bulletin* **79**: 7531–7554.

[38] Senthil R. A., Theerthagiri J. and Madhavan J. (2015) Hematite Fe_2O_3 Nanoparticles Incorporated Polyvinyl Alcohol Based Polymer Electrolytes for Dye-Sensitized Solar Cells. *Materials Science Forum* **832**: 72-83.

[39] Shashikala B.S., Murad Q.A. A., Fares H. A., Nabil A., Ahmed B., Siddaramaiah, and Anasuya S. J. (2022) Probing Optical Efficiency and Electrochemical Behaviors of Polycarbonate Incorporating Conducting PANI and Halloysite Nanotube (HNTs) as Core-Sell Nanofillers, *Polymer Bulletin* **79**: 10333-10355.